ACS APPLIED MATERIALS & INTERFACES

Research Article

www.acsami.org

Visual Detection of Multiplex MicroRNAs Using Cationic Conjugated Polymer Materials

Yuanyuan Zhou,[†] Jiangyan Zhang,[†] Likun Zhao,[†] Yingcun Li,[†] Hui Chen,[‡] Shengliang Li,[‡] and Yongqiang Cheng*[,†]

[†]Key Laboratory of Medicinal Chemistry and Molecular Diagnosis, Ministry of Education, Key Laboratory of Analytical Science and Technology of Hebei Province, College of Chemistry and Environmental Science, Hebei University, Baoding 071002, Hebei, P. R. China

[‡]Key Laboratory of Organic Solids, Institute of Chemistry, Chinese Academy of Sciences, Beijing 100190, P. R. China

Supporting Information

ABSTRACT: A simple, visual, and specific method for simultaneous detection of multiplex microRNAs (miRNAs) has been developed by integrating duplex-specific nuclease (DSN)-induced amplification with cationic conjugated polymer (CCP) materials. The probe DNA with a complementary sequence to target miRNA is labeled with fluorescein dye (FAM). Without target miRNA, the single-strand DNA probe cannot be digested by DSN. Upon adding CCPs, efficient fluorescence resonance energy transfer (FRET) from CCP to FAM occurs owing to strong electrostatic interactions between CCP and the DNA probe. In the presence of target miRNA, the DNA probe hybridizes with target miRNA followed by digestion to small nucleotide fragments by DSN; meanwhile, the miRNA is released and subsequently interacts again with the probe, resulting in the cycled digestion of the DNA probe. In this case, weak electrostatic interactions between oligonucleotide fragments and CCP lead to inefficient FRET from CCP to FAM. Thus, by triggering the FRET signal from CCP to FAM, miRNA can be specially detected, and the fluorescence color change based on FRET can be visualized directly with the naked eye under an UV lamp. Furthermore, an energy transfer cascade can be designed using CCP and DNA probes labeled at the 5′-terminus with FAM and Cy3 dyes, and the multistep FRET processes offer the ability of simultaneous detection of multiplex miRNAs.

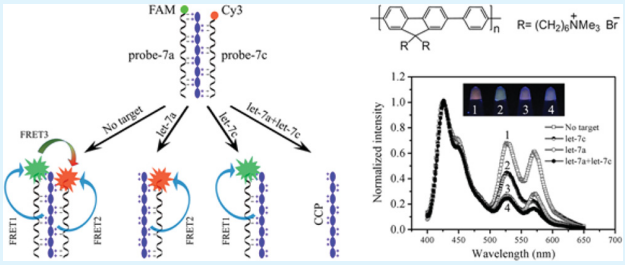

KEYWORDS: *cationic conjugated polymer, microRNA, FRET, multiplex detection, visual detection*

INTRODUCTION

MicroRNAs (miRNAs) are small noncoding RNAs with about 22 nucleotides and play key roles in various biological processes and diseases.[1,2] MiRNAs have emerged as a class of novel biomarkers, and many studies have shown that the expression levels of miRNAs are closely related to many of the human diseases, especially cancer.[3−5] Thus, it is vital to develop a simple, rapid, and sensitive miRNA detection method for further understanding of the biological functions of miRNAs, early diagnosis and treatment of diseases, and the development of gene drugs, etc.[6] Up to date, a variety of methods have been developed for detection of miRNAs,[7,8] while each method exhibits its advantages and disadvantages. Northern blotting is used as a golden level in the miRNA detection; however, the low sensitivity and complex procedures limit its wide application.[9,10] Direct colorimetric detection of miRNA was reported with a visual readout signal and simple processes based on the comformational change of the cationic polythiophene derivative[11] or the aggregation of gold nanoparticles.[12] Nevertheless, it is not satisfactory due to the poor sensitivity and multiplicity. To improve the sensitivity of miRNA detection, many amplification techniques were employed, such as polymerase chain reaction (PCR),[13−15] rolling circle amplification (RCA),[16−18] strand displacement amplification (SDA),[19,20] and ligase chain reaction (LCR),[21,22] etc. However, the amplification detections usually need high precision instruments and sophisticated operations. Additionally, considering that a kind of biological function or disease may be closely associated with various miRNAs, it is necessary to perform the multiplex miRNA detection simultaneously. Although the microarray chip can fulfill the high-throughput detection of miRNAs,[23,24] its sensitivity and specificity is low, and its cost is considerable. Some separation techniques, such as capillary electrophoresis and microparticles, have been applied to detection of various miRNAs.[22,25,26] The separation-based methods are, however, not fit for the routine miRNA detection because of the sophisticated equipment, expensive reagents, and the time-consuming processes. As a result, the

Received: November 17, 2015
Accepted: December 28, 2015
Published: December 28, 2015

DOI: 10.1021/acsami.5b11135
ACS Appl. Mater. Interfaces 2016, 8, 1520−1526

simple, sensitive, and multiplex detection of miRNAs still faces challenges.

Recently, duplex-specific nuclease (DSN) is applied in detection of miRNA with its unique feather that degrades not only double-stranded DNA but also DNA in the DNA−RNA hybrid.[27−29] Meanwhile, DSN has no activity to single-strand DNA and RNA. Thus, DSN is well suitable for detection of miRNA based on its characteristic of cleavage of DNA in the DNA−miRNA heteroduplex. After cleavage, miRNA is released and can subsequently hybridize with the remaining DNA to form a new heteroduplex. Then DSN can keep cleaving the DNA in the heteroduplex and repeating the hybridization/cleavage cycle, producing signal amplification. Furthermore, it is important that various probes can be designed and used to detect multiple miRNAs by DSN simultaneously. Yin et al. employed DSN to digest the TaqMan probes, which released and recycled target miRNAs for multiplex detection of miRNAs.[29] Yang et al. synthesized the 2-OMe-RNA modified molecular beacon probe and developed a target recycling amplification method based on DSN for highly sensitive and selective miRNA detection.[30] However, the TaqMan probes and the modified molecular beacons used in the methods were usually complex and costly, and the TaqMan probe-based assay only differs by at least four bases in miRNA sequences, which limits the distinction of homologous miRNAs with single-base differences. Therefore, to further develop the novel, simple, and multiplex detection of miRNAs based on DSN is still desired.

Cationic conjugated polymers (CCPs) with their powerful light-harvesting and signal amplification abilities provide a versatile detection platform for bioanalysis and biosensing.[31−33] Water-soluble CCPs as optical probes have increasingly been developed through the colorimetric and fluorometric assay for metal ions, proteins, and nucleic acids, etc.[34−39] Typically, CCPs are easy to bind with negatively charged nucleic acids via electrostatic interactions. Therefore, efficient fluorescence resonance energy transfer (FRET) can occur from CCPs to fluorophores labeled in oligonucleotide probes, which advances many homogeneous and sensitive nucleic acid detections. More importantly, CCPs can not only carry out multiplex detection of nucleic acids based on the multiple FRET from CCPs to various fluorescence dyes but also directly perform visual detection of the fluorescence signals by using a hand-held UV lamp.[40−43]

Herein, we develop a novel assay for detection of miRNAs by combining DSN-assisted amplification with homogeneous multiplex biosensing of CCPs. First, fluorescence-probe-labeled dyes including fluorescein and Cy3 are designed with the complementary sequences to the corresponding target miRNAs. When CCPs are added, efficient FRETs from CCPs to fluorescence probes can occur owing to the strong electrostatic interaction between CCPs and probes, and the color fluorescence signal can be directly observed under UV lamp irradiation. In the presence of DSN, the fluorescence probes complementary to the target miRNAs are digested to small oligonucleotide fragments by DSN, while the target miRNAs are released and subsequently hybridized with the new fluorescence probes, resulting in the cycled digestion of the fluorescence probes. After the probes are digested, the electrostatic interactions between fluorophore-labeled oligonucleotide fragments and CCPs are weak so that efficient FRET from CCPs to fluorophores does not take place. When the reaction solution is exposed to an UV lamp, only the self-fluorescence signal of CCPs is observed. Thus, the multiplex and visual detection of miRNAs can be realized by using DSN and CCPs.

EXPERIMENTAL SECTION

Materials and Reagents. Duplex-specific nuclease (DSN) was purchased from Evrogen Joint Stock Company (Russia). The RiboLock™ RNase Inhibitor was purchased from Fermentas. 4-(2-Hydroxyethyl)-1-piperazineethanesulfonic acid (HEPES) was obtained from Sigma. The cationic poly[(9,9-bis(6′-*N*,*N*,*N*-trimethylammonium)hexyl) fluorenylene phenylene dibromide] used as the CCP in the FRET experiments was prepared as described in the literature.[38] All the oligonucleotides purified by HPLC were synthesized by TaKaRa Biotechnology Co., Ltd. (Dalian, China). The sequences of the probes and targets are listed in Table S1. The reaction solution of miRNA was prepared by DEPC-treated water. All the chemicals were of analytical grade and used as purchased without further purification.

Instruments. The reaction was performed in a 2720 thermal cycler (Applied Biosystems, USA). A Hitachi F-4500 spectrofluorometer (Tokyo, Japan) equipped with a xenon lamp was used to determine the fluorescence intensity of the fluorescence spectra of the solution. Nikon D90 was used to record the color change with CCPs that showed the degree of integration.

DSN-Assisted Amplification of miRNA. The amplification reaction was performed in a 10 μL mixture, which contained 50 mM Tris-HCl (pH = 8.0), 5 mM $MgCl_2$, 1 mM DTT, 50 nM probe-7a, 8 U RNase Inhibitor, 0.5 U DSN, and the appropriate amount of target miRNA. The mixture was heated to 65 °C for 2 min and then incubated for 4 h at 45 °C in a 2720 thermal cycler.

Fluorescence Measurement by Using CCPs. Aliquots of 4 μL of the above products and 4 μL of CCP (15 μM) were then transferred to a 200 μL centrifuge tube and diluted to a final volume of 200 μL with 25 mmol/L of HEPES buffer (pH 8.0). The fluorescence spectra were measured by a Hitachi F-4500 spectrofluorometer whose slit width for excitation and emission and PMT voltage were 5 nm and 700 V, respectively. The emission spectra were measured in the wavelength range of 400−650 nm with the excitation of 380 nm.

Visual Fluorescence Detection of miRNAs. The 10 μL reaction solution containing 50 nM probe-7a or probe-7c, 0.5 U DSN, and the different concentration of miRNAs was put through an amplification reaction as described above. Afterward, the reaction solution was mixed with 2 μL of CCP (15 μM). After incubation of 5 min, a hand-held UV lamp with the wavelength of 365 nm was used to excite the solution. The photograph with different color of the solution was taken by a Nikon D90 digital camera.

Extraction of Small RNAs from Hela Cells. Hela cells were cultivated in DMEM medium (GIBCO) containing 10% (v/v) fetal bovine serum (FBS). Small RNA was extracted with RNAiso for small RNA (Takara Biotechnology, Dalian). The extracted RNA was quantitated through the A260 value by a UV−vis spectrophotometer and stored at −80 °C.

Multiplex Detection of miRNAs with CCP in the Mixed Samples. To simulate the practical sample detection, we mixed equal amounts of the let-7b, let-7d, and miR221 with target miRNAs let-7a or/and let-7c to prepare the mixed samples. Each of miRNAs was 20 nM in 10 μL mixed samples, which included the mixed probes of 50 nM probe-7a and probe-7c, respectively. Fluorescence spectra were measured as described above. For visual miRNA detection in the mixed sample, 2 μL of 15 μM CCP was added to the solution and incubated for 5 min. The color of solution excited by a hand-held UV lamp was recorded with a Nikon D90 digital camera.

RESULTS AND DISCUSSION

Principle of miRNA Detection. The principle of miRNA detection by DSN and CCP is shown in Figure 1. The fluorophore-labeled oligonucleotide probe is designed and completely complementary to target miRNA. In the presence of the target miRNA, the fluorophore-labeled probe can hybridize

DOI: 10.1021/acsami.5b11135
ACS Appl. Mater. Interfaces 2016, 8, 1520−1526

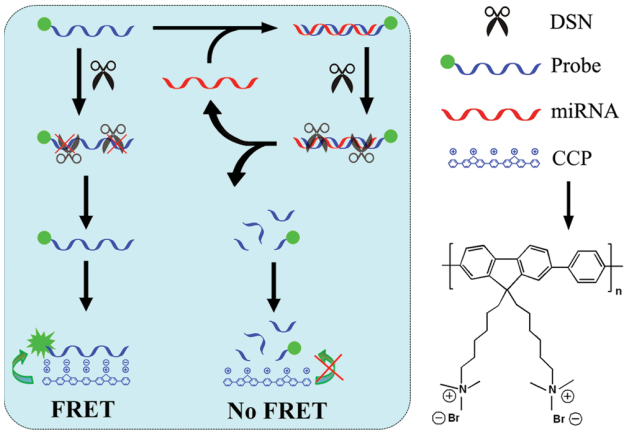

Figure 1. Principle of miRNA detection by DSN-assisted amplification and CCP biosensing.

with target miRNA to form a double-stranded miRNA−DNA complex. Afterward, the fluorophore-labeled probe is degraded to small oligonucleotide fragments by DSN, which prefers to hydrolyze DNA in DNA−RNA hybrid duplexes rather than ssDNA. At the same time, target miRNA is released and subsequently hybridizes with the other fluorophore-labeled probe, leading to the cyclic degradation reaction by DSN. As a result, target miRNA is replicated and amplified, while a large number of fluorophore-labeled oligonucleotide fragments are generated. When adding the CCP, efficient FRET cannot occur due to the weak electrostatic interaction between CCP and fluorophore-labeled oligonucleotide fragments. By comparison, without miRNA, the single-stranded fluorophore-labeled probe cannot be degraded by DSN and then bind with CCP through strong electrostatic interaction between negatively charged DNA and CCP, which bring them close to each other, resulting in efficient FRET from CCP to the fluorophore upon exciting CCP.

To verify the principle of the assay, let-7a was first chosen as the target miRNA. Down-regulation of let-7a is a key event in lung cancer, so let-7a is an important biomarker to be detected.[44] As shown in Figure 2, the FAM-labeled probe (probe-7a) is designed and completely complementary to let-7a. The fluorescence signal of CCP at 423 nm and that of FAM

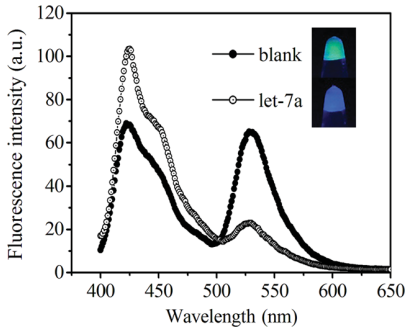

Figure 2. Fluorescence spectra of the reaction product after mixing with CCP. The DSN amplification products were diluted 50-fold with HEPES buffer (25 mM, pH = 8.0) before the fluorescence detection. Let-7a and CCP were 200 pM and 0.3 μM, respectively. Inlet is the visual fluorescence images of the assay solution under 365 nm UV irradiation. Sequential detections were carried out as described in the Experimental Section.

at 530 nm are remarkably observed in blank solution. This can be attributed to the fact that probe-7a can interact with CCP through strong electrostatic forces and lead to efficient FRET from CCP to FAM in probe-7a. Under 365 nm UV light irradiation, the green fluorescence from FAM in the assay solution was observed with the naked eye only. In contrast, in the sample solution containing let-7a, the fluorescence signal of CCP at 423 nm was obviously enhanced; meanwhile, the fluorescence signal of FAM in 530 nm was clearly reduced. This is because probe-7a hybridizes with let-7a to form the RNA−DNA complex. Probe-7a in the RNA−DNA complex is hydrolyzed to small oligonucleotide fragments by DSN. Thus, inefficient FRET from CCP to FAM takes place stemming from the weak electrostatic interaction between CCP and small oligonucleotide fragments. Only blue fluorescence from CCP in solution was observed under 365 nm UV light irradiation. We defined the ratio of fluorescence intensity at 423 and 530 nm as the fluorescence quenching efficiency ($I_{423\ nm}/I_{530\ nm}$). Therefore, it is possible to detect miRNA by measuring the fluorescence quenching efficiency or directly observing the different color of the reaction solution.

Specificity of the Assay. The experimental conditions including the concentration of probe and DSN, reaction time, and reaction temperature were studied and optimized as shown in the Supporting Information. To investigate the specificity of the method, we select miR221 and let-7 miRNA family, which are detected by using let-7a as the target miRNA and probe-7a as the specific probe. The sequences of miRNAs and probes are shown in Table S1. The let-7 miRNA family including let-7a, let-7b, let-7c, let-7d, let-7e, let-7f, and let-7g is a highly homologous miRNA whose sequences differ by only one or two nucleotides. It is important to specifically detect the let-7 miRNA family for understanding their biological functions. As shown in Figure 3, we can clearly discriminate let-7a from other

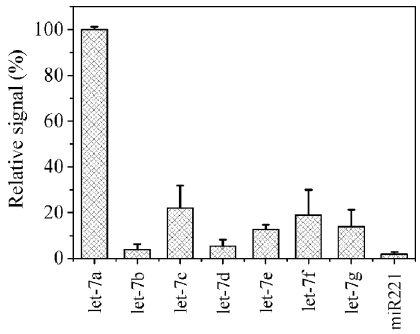

Figure 3. Relative signals of let-7 miRNA family members and miR221. The relative signals (%) denoted the ratio of the $I_{423\ nm}/I_{530\ nm}$ signal of each miRNA to the $I_{423\ nm}/I_{530\ nm}$ signal of let-7a. The relative fluorescence ratio signal of let-7a was normalized to be 100%. The concentration of each of the miRNAs was 40 pM. Sequential detections were carried out as described in the Experimental Section. Error bars were estimated from three replicate measurements.

miRNAs, indicating the high specificity of the proposed method. It is noteworthy that let-7c with the maximum nonspecific signals is due to the different base G in let-7c as compared with base A in let-7a in the same site near the 3′-terminus. What is more, the similar interaction energy between T-G and T-A incurs that let-7c is relatively difficult to be discriminated from let-7a.

DOI: 10.1021/acsami.5b11135
ACS Appl. Mater. Interfaces 2016, 8, 1520−1526

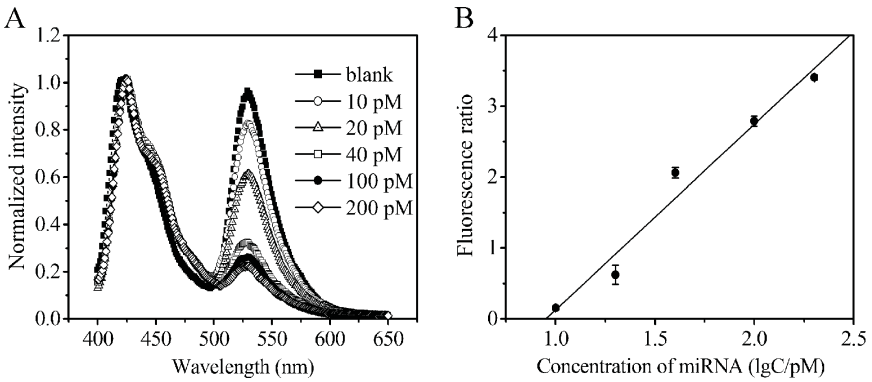

Figure 4. Dynamic range and sensitivity of the let-7a assay: (A) fluorescence spectra with a different amount of let-7a. The concentration of let-7a successively is 0, 10, 20, 40, 100, and 200 pM. (B) The relationship between fluorescence ratio and log of let-7a concentration. Each reaction was run in triplicate.

Dynamic Range and the Visual miRNA Detection of the Assay. To investigate the dynamic range for miRNA detection, the emission spectra of a series of amplification products with various concentrations of let-7a were measured upon adding CCP with the excitation at 380 nm (Figure 4A). As shown in Figure 4B, the FRET ratio ($I_{423\ nm}/I_{530\ nm}$) is a function of let-7a concentration. There is a good correlative relationship between the FRET ratio and the logarithm of let-7a concentration in the range of 10−200 pM. The linear function was $I_{423\ nm}/I_{530\ nm} = -2.487 + 2.616\ \lg(C/pM)$ with a correlation coefficient of $R = 0.9850$. Thus, the concentration of the miRNA would be quantitatively determined by measuring the FRET ratios. The detection limit (3s, $n = 11$) was estimated to be 4.6 pM. A series of seven repetitive measurements of 40 pM let-7a were used to evaluate the precision, and the relative standard deviation (RSD) was 3.7%.

To further simplify the miRNA detection, the fluorescent visual detection of miRNA was studied by using a hand-held UV lamp. As shown in Figure 5A, the different samples were directly detected with the naked eye under 365 nm UV light irradiation. For the FAM-labeled probe-7a, no visual signal is observed under UV light irradiation because the concentration of probe-7a is low (tube 1). Nevertheless, tube (2), which is the probe-7a solution as the blank, shows green color by adding CCP, originating from the efficient FRET from CCP to FAM and the excellent signal amplification ability of CCP. When let-7a at different concentration is introduced into the reaction solution, probe-7a hybridizes with let-7a and is degraded by DSN. Thus, upon addition of CCP, the FRET from CCP to FAM is gradually reduced with the increasing concentration of let-7a, giving rise to deep green, light green, and light blue color in tubes (3), (4), and (5), respectively.

To investigate the applicability of the method, a real sample of miRNA extracted in Hela cells is detected by visual detection. As shown in Figure 5A, the miRNA sample and probe-7a were mixed in tube (6) and processed through DSN-assisted CCP visual detection. In contrast with the green color in tube (2), the light blue color in tube (6) is observed, which is weaker than the dark blue color in tube (8) with CCP only under UV irradiation, suggesting that the weak FRET from CCP to FAM occurs and let-7a exists in the sample. Moreover, by introduction of the synthesized let-7a to the sample, the color of the reaction solution in tube (7) exhibits dark blue as compared with that of tube (8), indicating that FRET from CCP to FAM in the sample solution is further reduced with the

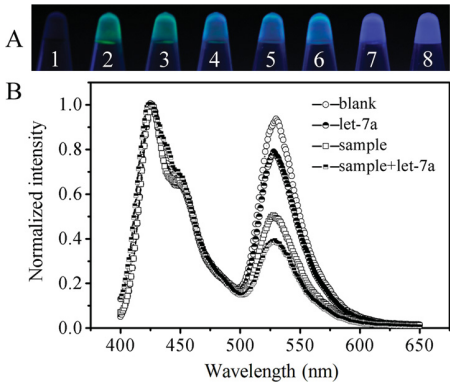

Figure 5. (A) Fluorescent visual detection of the different samples by a hand-held UV lamp. 1. Probe-7a; 2. CCP + probe-7a; 3. CCP + probe-7a + let-7a (0.5 nM); 4. CCP + probe-7a + let-7a (2 nM); 5. CCP + probe-7a + let-7a (10 nM); 6. CCP + probe-7a + real sample (1.0 μg); 7. CCP + probe-7a + real sample (1.0 μg) + let-7a (0.5 nM); 8. CCP. The visual fluorescence detection was carried out as described in the Experimental Section. (B) Fluorescence spectra of the real sample and synthesized let-7a. The curves from top to bottom orderly come from the corresponding samples of tubes (2), (3), (6), and (7) in (A). The concentrations of probe-7a and let-7a were 1 nM and 10 pM, respectively. Fluorescence measurements were carried out as described in the Experimental Section.

increasing of the concentration of let-7a in reaction solution. These results are in accord with those of fluorescence spectra in Figure 5B, indicating that the method has good applicability.

Multiplex Detection of miRNAs. To study the multiplex detection of miRNA by the method, we designed a new Cy3-labeled probe (probe-7c) with a complementary sequence of let-7c for detection of let-7c based on the high specificity of the method. As shown in Figure 6, for the blank solution, the fluorescence signals of Cy3 at 570 nm are relatively high because probe-7c interacts with CCP through strong electrostatic forces leading to efficient FRET from CCP to Cy3 in probe-7c. So, under UV irradiation, the blank solution shows reddish brown color derived from Cy3. In the presence of let-7c, the FRET from CCP to Cy3 is obviously reduced, and the solution exhibits purple color under UV irradiation. This is due to the fact that probe-7c hybridizes with let-7c to form the RNA−DNA complex. As the probe-7a, probe-7c in the RNA−DNA complex is also hydrolyzed by DSN, resulting in inefficient FRET from CCP to Cy3. Therefore, the fluorescence

DOI: 10.1021/acsami.5b11135
ACS Appl. Mater. Interfaces 2016, 8, 1520−1526

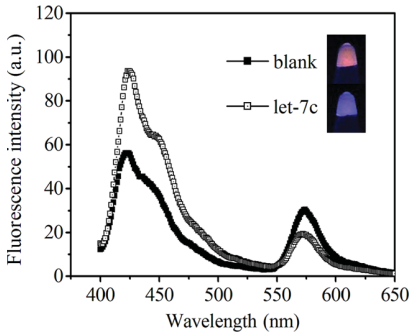

Figure 6. Fluorescence spectra of the let-7c reaction product after mixing with CCP. The DSN amplification products were diluted 50-fold with HEPES buffer (25 mM, pH = 8.0) before the fluorescence detection. Let-7c and CCP were 200 pM and 0.3 μM, respectively. Probe-7c was labeled with Cy3, and the maximum emission wavelength of Cy3 was 570 nm. Inlet is the visual fluorescence images of the assay solution under 365 nm UV irradiation. Sequential detection was carried out as described in the Experimental Section.

quenching efficiency ($I_{423\ nm}/I_{570\ nm}$) can be defined as the ratio of fluorescence intensity at 423 and 570 nm and used to measure miRNA. Moreover, the result can be directly observed by the color changes of reaction solution.

To demonstrate the multiplex detection of the method, we mixed the probe-7a with the probe-7c to form the mixed probes, which were suitable for the various samples with DSN-assisted CCP multiplex biosensing. The principle scheme of multiplex detection of miRNAs by the mixed probes is shown in Figure 7. If no target miRNAs exist, both probe-7a and

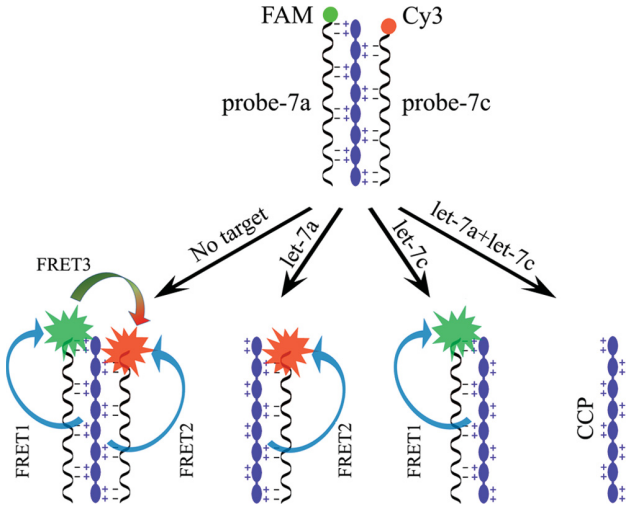

Figure 7. Principle of multiplex detection of miRNAs by the mixed probes.

probe-7c in the mixed probes interact with CCP through the strong electrostatic force and subsequently bring about FRET1 and FRET2 from CCP to FAM and Cy3, respectively. Furthermore, FRET3 from FAM to Cy3 is also simultaneously triggered due to the proximity distance and the suitable molecular structure of FAM and Cy3. If the sample has let-7a and no let-7c, only probe-7a hybridizes with let-7a and is degraded by DSN. Thus, no FRET1 and FRET3 are initiated, and only FRET2 takes place. By contrast, when let-7c exists in the sample, based on a similar reaction mechanism, only probe-7c is degraded, leading to FRET1 only and inefficient FRET2 and FRET3. When the sample includes let-7a and let-7c, probe-7a and probe-7c interact with let-7a and let-7c, respectively, and all of the mixed probes are degraded by DSN, leading to any inefficient FRET in the reaction solution.

Figure 8 shows the fluorescence spectra and the visual images of the various samples, which verify the multiplex detection

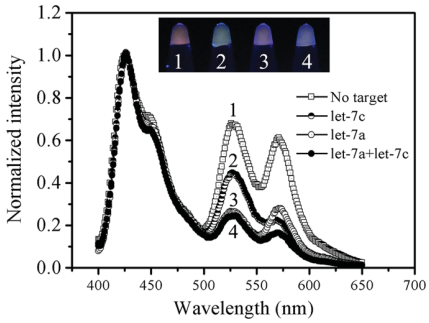

Figure 8. Fluorescence spectra and visual images of various samples for multiplex detection of miRNAs by the mixed probes. Sequential detection was carried out as described in the Experimental Section.

principle for miRNAs. As there are not target miRNAs, curve (1) shows the clearly fluorescence peaks of FAM and Cy3 in 530 and 570 nm, respectively. Correspondingly, inset (1) appears as a brown color that is the mixed color of FAM and Cy3. These results are attributed to the facts that the mixed probes interact with CCP and the multiple FRETs from CCP to FAM and Cy3 and from FAM to Cy3 take place, respectively. In curve (2), only let-7c in the sample, the fluorescence peak at 570 nm is significantly reduced, while the fluorescence peak at 530 nm is still high. Accordingly, the light green color is observed in inlet (2). This can be explained by the fact that probe-7c in the mixed probes hybridizes with let-7c and is degraded to the small nucleotide fragments by DSN, resulting in inefficient FRET from CCP or FAM to Cy3. At the same time, probe-7a in the mixed probes interacts with CCP, and efficient FRET from CCP to FAM takes place. Compared with curve (2), curve (3) with let-7a displays the distinctly reduced fluorescence signal at 530 nm and the relatively prominent fluorescence peak at 570 nm, and inlet (3) shows the light rufous color. This is attributed to the same mechanism as let-7c that probe-7a hybridizes with let-7a and is degraded by DSN, generating inefficient FRET from CCP to FAM, and probe-7c in the mixed probes interacts with CCP only, giving rise to efficient FRET from CCP to Cy3. Similarly, for the sample with let-7a and let-7c simultaneously, as shown in curve 4, the fluorescence signals in 530 and 570 nm are reduced markedly. And nattier blue is observed in inlet (4). This is due to that probe-7a and probe-7c, respectively, interact with let-7a and let-7c and undergo the degradation reaction synchronously by DSN, leading to inefficient FRETs from CCP to FAM and Cy3. Therefore, the different miRNAs, which even differ by one base, can be discriminated from the different mixed samples with the visual detection by the mixed probes, indicating that multiplex detection of miRNAs can be achieved by the proposed method.

CONCLUSION

A simple, visual, and specific method for simultaneous detection of multiplex microRNAs has been developed by

DOI: 10.1021/acsami.5b11135
ACS Appl. Mater. Interfaces 2016, 8, 1520−1526

integrating DSN-induced amplification with CCP materials. Compared with miRNA detection and CCP-based biosensing methods reported previously, the proposed method has several unique advantages. First, the assay integrates isothermal DSN-induced DNA amplification with CCP biosensing, which ensures miRNAs detection with the high sensitivity and specificity in a homogeneous fashion. Second, multiplex detection of miRNAs can be achieved successfully, resulting from the CCP-based multiple FRET and excellent signal amplification ability of CCP. Third, the result can be directly observed by the naked eye under only a hand-held UV lamp, which is simple and convenient. As a result, the method not only further expands the applicability of conjugated polymers but also paves a new avenue for multiplex detection of nucleic acids and clinical diagnosis.

■ ASSOCIATED CONTENT

Supporting Information

The Supporting Information is available free of charge on the ACS Publications website at DOI: 10.1021/acsami.5b11135.

Optimization of experimental conditions and the sequences of the oligonucleotides and miRNAs used in the experimental study (PDF)

■ AUTHOR INFORMATION

Corresponding Author

*E-mail: yqcheng@hbu.edu.cn. Tel./Fax: +86-312-5079403.

Author Contributions

The manuscript was written through contributions of all authors. All authors have given approval to the final version of the manuscript.

Notes

The authors declare no competing financial interest.

■ ACKNOWLEDGMENTS

The authors are grateful for the financial support of the National Natural Science Foundation of China (No. 21475031), the Natural Science Foundation of Hebei Province, China (No. B2012201078), and Postdoctoral Science Foundation of China (Nos. 2013M540144 and 2014T70124).

■ REFERENCES

(1) Bartel, D. P. MicroRNA: Genomics, Biogenesis, Mechanism, and Function. *Cell* **2004**, *116*, 281−297.
(2) Alvarez-Garcia, I.; Miska, E. A. MicroRNA Functions in Animal Development and Human Disease. *Development* **2005**, *132*, 4653−4662.
(3) Fabian, M. R.; Sonenberg, N.; Filipowicz, W. Regulation of mRNA Translation and Stability by Micrornas. *Annu. Rev. Biochem.* **2010**, *79*, 351−379.
(4) Calin, G. A.; Croce, C. M. MicroRNA Signatures in Human Cancers. *Nat. Rev. Cancer* **2006**, *6*, 857−866.
(5) Hayes, J.; Peruzzi, P. P.; Lawler, S. MicroRNA in Cancer: Biomarkers, Functions and Therapy. *Trends Mol. Med.* **2014**, *20*, 460−469.
(6) Cheng, G. Circulating MiRNAs: Roles in Cancer Diagnosis, Prognosis and Therapy. *Adv. Drug Delivery Rev.* **2015**, *81*, 75−93.
(7) Dong, H.; Lei, J.; Ding, L.; Wen, Y.; Ju, H.; Zhang, X. MicroRNA: Function, Detection, and Bioanalysis. *Chem. Rev.* **2013**, *113*, 6207−6233.
(8) Hunt, E. A.; Broyles, D.; Head, T.; Deo, S. K. MicroRNA Detection: Current Technology and Research Strategies. *Annu. Rev. Anal. Chem.* **2015**, *8*, 217−237.
(9) Lau, N. C.; Lim, L. P.; Weinstein, E. G.; Bartel, D. P. An Abundant Class of Tiny RNAs with Probable Regulatory Roles in Caenorhabditis Elegans. *Science* **2001**, *294*, 858−862.
(10) Sempere, L. F.; Freemantle, S.; Pitha-Rowe, I.; Moss, E.; Dmitrovsky, E.; Ambros, V. Expression Profiling of Mammalian MicroRNAs Uncovers a Subset of Brain-Expressed Micrornas with Possible Roles in Murine and Human Neuronal Differentiation. *Genome Biol.* **2004**, *5*, R13.
(11) Zhang, Y.; Li, Z.; Cheng, Y.; Lv, X. Colorimetric Detection of MicroRNA and RNase H Activity in Homogeneous Solution with Cationic Polythiophene Derivative. *Chem. Commun.* **2009**, 3172−3174.
(12) Park, J.; Yeo, J.-S. Colorimetric Detection of MicroRNA miR-21 Based on Nanoplasmonic Core−Satellite Assembly. *Chem. Commun.* **2014**, *50*, 1366−1368.
(13) Chen, C.; Ridzon, D. A.; Broomer, A. J.; Zhou, Z.; Lee, D. H.; Nguyen, J. T.; Barbisin, M.; Xu, N. L.; Mahuvakar, V. R.; Andersen, M. R. Real-Time Quantification of MicroRNAs by Stem−Loop RT−PCR. *Nucleic Acids Res.* **2005**, *33*, e179.
(14) Zhang, J.; Li, Z.; Wang, H.; Wang, Y.; Jia, H.; Yan, J. Ultrasensitive Quantification of Mature MicroRNAs by Real-Time PCR Based on Ligation of a Ribonucleotide-Modified DNA Probe. *Chem. Commun.* **2011**, *47*, 9465−9467.
(15) Wang, P.; Jing, F.; Li, G.; Wu, Z.; Cheng, Z.; Zhang, J.; Zhang, H.; Jia, C.; Jin, Q.; Mao, H.; et al. Absolute Quantification of Lung Cancer Related MicroRNA by Droplet Digital PCR. *Biosens. Bioelectron.* **2015**, *74*, 836−842.
(16) Cheng, Y.; Zhang, X.; Li, Z.; Jiao, X.; Wang, Y.; Zhang, Y. Highly Sensitive Determination of MicroRNA Using Target-Primed and Branched Rolling-Circle Amplification. *Angew. Chem., Int. Ed.* **2009**, *48*, 3268−3272.
(17) Li, Y.; Liang, L.; Zhang, C. Isothermally Sensitive Detection of Serum Circulating MiRNAs for Lung Cancer Diagnosis. *Anal. Chem.* **2013**, *85*, 11174−11179.
(18) Deng, R.; Tang, L.; Tian, Q.; Wang, Y.; Lin, L.; Li, J. Toehold-Initiated Rolling Circle Amplification for Visualizing Individual MicroRNAs in Situ in Single Cells. *Angew. Chem., Int. Ed.* **2014**, *53*, 2389−2393.
(19) Zhang, L.; Zhu, G.; Zhang, C. Homogeneous and Label-Free Detection of MicroRNAs Using Bifunctional Strand Displacement Amplification-Mediated Hyperbranched Rolling Circle Amplification. *Anal. Chem.* **2014**, *86*, 6703−6709.
(20) Chen, A.; Gui, G.; Zhuo, Y.; Chai, Y.; Xiang, Y.; Yuan, R. Signal-Off Electrochemiluminescence Biosensor Based on Phi29 DNA Polymerase Mediated Strand Displacement Amplification for MicroRNA Detection. *Anal. Chem.* **2015**, *87*, 6328−6334.
(21) Zhang, P.; Liu, Y.; Zhang, Y.; Liu, C.; Wang, Z.; Li, Z. Multiplex Ligation-Dependent Probe Amplification (MLPA) for Ultrasensitive Multiplexed MicroRNA Detection Using Ribonucleotide-Modified DNA Probes. *Chem. Commun.* **2013**, *49*, 10013−10015.
(22) Zhang, P.; Zhang, J.; Wang, C.; Liu, C.; Wang, H.; Li, Z. Highly Sensitive and Specific Multiplexed MicroRNA Quantification Using Size-Coded Ligation Chain Reaction. *Anal. Chem.* **2014**, *86*, 1076−1082.
(23) Castoldi, M.; Schmidt, S.; Benes, V.; Hentze, M. W.; Muckenthaler, M. U. MiChip: An Array-Based Method for MicroRNA Expression Profiling Using Locked Nucleic Acid Capture Probes. *Nat. Protoc.* **2008**, *3*, 321−329.
(24) Lee, J. M.; Jung, Y. Two-Temperature Hybridization for Microarray Detection of Label-Free MicroRNAs with Attomole Detection and Superior Specificity. *Angew. Chem., Int. Ed.* **2011**, *50*, 12487−12490.
(25) Chapin, S. C.; Appleyard, D. C.; Pregibon, D. C.; Doyle, P. S. Rapid MicroRNA Profiling on Encoded Gel Microparticles. *Angew. Chem., Int. Ed.* **2011**, *50*, 2289−2293.
(26) Wegman, D. W.; Ghasemi, F.; Khorshidi, A.; Yang, B. B.; Liu, S. K.; Yousef, G. M.; Krylov, S. N. Highly-Sensitive Amplification-Free Analysis of Multiple MiRNAs by Capillary Electrophoresis. *Anal. Chem.* **2014**, *87*, 1404−1410.

DOI: 10.1021/acsami.5b11135
ACS Appl. Mater. Interfaces 2016, 8, 1520−1526

(27) Shagin, D. A.; Rebrikov, D. V.; Kozhemyako, V. B.; Altshuler, I. M.; Shcheglov, A. S.; Zhulidov, P. A.; Bogdanova, E. A.; Staroverov, D. B.; Rasskazov, V. A.; Lukyanov, S. A Novel Method for SNP Detection Using a New Duplex-Specific Nuclease from Crab Hepatopancreas. *Genome Res.* **2002**, *12*, 1935−1942.
(28) Nilsen, I. W.; Øverbø, K.; Havdalen, L. J.; Elde, M.; Gjellesvik, D. R.; Lanes, O. The Enzyme and the cDNA Sequence of a Thermolabile and Double-Strand Specific DNase from Northern Shrimps (Pandalus Borealis). *PLoS One* **2010**, *5*, e10295.
(29) Yin, B. C.; Liu, Y. Q.; Ye, B. C. One-Step, Multiplexed Fluorescence Detection of MicroRNAs Based on Duplex-Specific Nuclease Signal Amplification. *J. Am. Chem. Soc.* **2012**, *134*, 5064−5067.
(30) Lin, X.; Zhang, C.; Huang, Y.; Zhu, Z.; Chen, X.; Yang, C. J. Backbone-Modified Molecular Beacons for Highly Sensitive and Selective Detection of MicroRNAs Based on Duplex Specific Nuclease Signal Amplification. *Chem. Commun.* **2013**, *49*, 7243−7245.
(31) Duan, X.; Liu, L.; Feng, F.; Wang, S. Cationic Conjugated Polymers for Optical Detection of DNA Methylation, Lesions, and Single Nucleotide Polymorphisms. *Acc. Chem. Res.* **2009**, *43*, 260−270.
(32) Zhu, C.; Liu, L.; Yang, Q.; Lv, F.; Wang, S. Water-Soluble Conjugated Polymers for Imaging, Diagnosis, and Therapy. *Chem. Rev.* **2012**, *112*, 4687−4735.
(33) Feng, L.; Zhu, C.; Yuan, H.; Liu, L.; Lv, F.; Wang, S. Conjugated Polymer Nanoparticles: Preparation, Properties, Functionalization and Biological Applications. *Chem. Soc. Rev.* **2013**, *42*, 6620−6633.
(34) Liang, J.; Li, K.; Liu, B. Visual Sensing With Conjugated Polyelectrolytes. *Chem. Sci.* **2013**, *4*, 1377−1394.
(35) Wu, Y.; Tan, Y.; Wu, J.; Chen, S.; Chen, Y. Z.; Zhou, X.; Jiang, Y.; Tan, C. Fluorescence Array-Based Sensing of Metal Ions Using Conjugated Polyelectrolytes. *ACS Appl. Mater. Interfaces* **2015**, *7*, 6882−6888.
(36) Wang, C.; Tang, Y.; Liu, Y.; Guo, Y. Water-Soluble Conjugated Polymer as a Platform for Adenosine Deaminase Sensing Based on Fluorescence Resonance Energy Transfer Technique. *Anal. Chem.* **2014**, *86*, 6433−6438.
(37) Wu, D.; Schanze, K. S. Protein Induced Aggregation of Conjugated Polyelectrolytes Probed with Fluorescence Correlation Spectroscopy: Application to Protein Identification. *ACS Appl. Mater. Interfaces* **2014**, *6*, 7643−7651.
(38) Li, F.; Chao, J.; Li, Z.; Xing, S.; Su, S.; Li, X.; Song, S.; Zuo, X.; Fan, C.; Liu, B.; Huang, W.; Wang, L.; Wang, L. Graphene Oxide-Assisted Nucleic Acids Assays Using Conjugated Polyelectrolytes-Based Fluorescent Signal Transduction. *Anal. Chem.* **2015**, *87*, 3877−3883.
(39) Feng, X.; Duan, X.; Liu, L.; Feng, F.; Wang, S.; Li, Y.; Zhu, D. Fluorescence Logic-Signal-Based Multiplex Detection of Nucleases with the Assembly of a Cationic Conjugated Polymer and Branched DNA. *Angew. Chem., Int. Ed.* **2009**, *48*, 5316−5321.
(40) Song, J.; Zhang, J.; Lv, F.; Cheng, Y.; Wang, B.; Feng, L.; Liu, L.; Wang, S. Multiplex Detection of DNA Mutations by the Fluorescence Fingerprint Spectrum Technique. *Angew. Chem., Int. Ed.* **2013**, *52*, 13020−13023.
(41) Duan, X.; Wang, S.; Li, Z. Conjugated Polyelectrolyte−DNA Complexes for Multi-Color and One-Tube SNP Genotyping Assays. *Chem. Commun.* **2008**, 1302−1304.
(42) Song, J.; Yang, Q.; Lv, F.; Liu, L.; Wang, S. Visual Detection of DNA Mutation Using Multicolor Fluorescent Coding. *ACS Appl. Mater. Interfaces* **2012**, *4*, 2885−2890.
(43) Duan, X.; Yue, W.; Liu, L.; Li, Z.; Li, Y.; He, F.; Zhu, D.; Zhou, G.; Wang, S. Single-Nucleotide Polymorphism (SNP) Genotyping Using Cationic Conjugated Polymers in Homogeneous Solution. *Nat. Protoc.* **2009**, *4*, 984−991.
(44) Johnson, S. M.; Grosshans, H.; Shingara, J.; Byrom, M.; Jarvis, R.; Cheng, A.; Labourier, E.; Reinert, K. L.; Brown, D.; Slack, F. J. *RAS* Is Regulated by the let-7 MicroRNA Family. *Cell* **2005**, *120*, 635−647.

DOI: 10.1021/acsami.5b11135
ACS Appl. Mater. Interfaces 2016, 8, 1520−1526